Plant Stress 18 (2025) 101113

Contents lists available at ScienceDirect

Plant Stress

journal homepage: www.sciencedirect.com/journal/plant-stress

Upcycling agricultural byproducts: Peach Peel Extract provides dual action protection against rice root-knot nematodes

Yaseen Ahmad [a], Karen De Kock [a], Kristof Demeestere [b], Muhammad Nauman Ahmad [c], Tim De Meyer [d], Susanne K. Wiedmer [e], Tina Kyndt [a,*]

[a] Department of Biotechnology, Faculty of Bioscience Engineering, Ghent University, Proeftuinstraat 86 B– 9000 Ghent, Belgium
[b] Department of Green Chemistry and Technology, Research Group EnVOC, Faculty of Bioscience Engineering, Ghent University, Coupure Links 653 B–9000 Ghent, Belgium
[c] Department of Agricultural Chemistry and Biochemistry, The University of Agriculture, Peshawar 25000 Peshawar, Pakistan
[d] Department of Data Analysis and Mathematical Modelling, Faculty of Bioscience Engineering, Ghent University, Ghent, Belgium
[e] Department of Chemistry, A. I. Virtasen Aukio 1, PO BOX 55, FIN-00014, University of Helsinki, Finland

ARTICLE INFO

Keywords:
Induced systemic resistance
Rice
Meloidogyne graminicola
ROS
Sustainability

ABSTRACT

Bioprotectants represent promising alternatives to chemical pesticides for sustainable agriculture. This study explores the bioprotective potential of extracts derived from agricultural byproducts of three Rosaceae family members, with particular focus on Peach Peel Extract (PPE). Results from this study demonstrate that PPE serves as an effective bioprotectant against the root-knot nematode *Meloidogyne graminicola* in rice through a sophisticated dual-action mechanism. The extract exhibits direct nematicidal activity against second-stage juveniles while simultaneously triggering systemic induction of plant immune pathways when applied as a foliar spray. This induced resistance phenotype is characterized by elevated phenolic and flavonoid levels and a reactive oxygen species (ROS) burst in local tissues, resulting in a systemic effect associated with significant reductions in gall formation, total nematode populations, and egg-laying females in rice roots. Through integrated phytohormone analysis, transcriptome profiling, and mutant studies, we identified the jasmonic acid (JA) pathway as essential for the induced resistance response. Multi-omics profiling revealed coordinated upregulation of JA and ROS signaling pathways alongside secondary metabolite biosynthesis, resulting in accumulation of key defense compounds including isothiocyanates, resveratrol, azelaic acid, and diterpene glycosides. These findings validate PPE as an effective bioprotectant and demonstrate the potential for transforming agricultural byproducts into sustainable crop protection solutions.

1. Introduction

The significance of implementing improved pest management strategies has continued to increase because of the ecological and regulatory obstacles encountered by traditional chemical methods (Kitowski et al., 2020). Although effective, traditional pesticides often exhibit broad spectrum toxicity, harming nontarget species, and disrupting ecosystems (Rani et al., 2021). Their extensive use has raised significant environmental concerns including pollution, pest resilience, and health hazards to humans and ecosystems. Consequently, the use of numerous commercial pesticides has been prohibited or restricted in many countries, urging the need to identify environmentally friendly alternatives.

Agricultural byproducts and waste streams could be excellent sources of bioactive compounds with bioprotectant activity. In many developing countries, such byproducts are indiscriminately dumped or burned in public places, leading to soil and air pollution. Residues from these activities can enter water bodies and pollute aquatic environments (Koul et al., 2022; Varma et al., 2015; Wang et al., 2016). Repurposing agricultural byproducts has the potential to mitigate environmental contamination and facilitate a circular economic framework. Plant-derived products, including botanical extracts and immune elicitors, have repeatedly shown dual benefits by directly suppressing pests and activating host defenses. For example, bioactivity has been described for allicin from garlic (Slusarenko et al., 2008), essential oils such as limonene and linalool from citrus peel (Assadpour et al., 2024), azadirachtin from neem, pyrethrins from chrysanthemum, and

* Corresponding author.
E-mail address: tina.kyndt@ugent.be (T. Kyndt).

https://doi.org/10.1016/j.stress.2025.101113
Received 4 August 2025; Received in revised form 22 October 2025; Accepted 26 October 2025
Available online 26 October 2025

protective Cucurbitaceae peel extracts (Ensley 2018; Shu et al., 2018; De Kesel et al., 2022).

Induced resistance (IR) presents an appealing and environmentally friendly crop protection strategy (Jamiołkowska 2020). IR reduces disease susceptibility by exposing plants to external stimuli, such as beneficial microbes (e.g. *Trichoderma spp*.), natural compounds (e.g. piperonylic acid and thiamine), and chemical compounds, such as synthetic analogues of salicylic acid (SA) (acibenzolar-S-methyl) (De Kesel et al., 2022; Desmedt et al., 2021; Martínez-Medina et al., 2017). IR involves direct defence induction and priming, which potentiates the subsequent defence responses of the plant. Exposure to IR stimulants induces both localised and systemic changes in gene expression and downstream physiological processes. These alterations encompass various cellular responses, including modifications in ion movement, production of secondary metabolites, strengthening of cell walls, and signalling through reactive oxygen species (ROS) (Conrath 2009; Desmedt et al., 2022).

IR has been demonstrated to be effective against numerous pests and pathogens, including plant parasitic nematodes. These nematodes constitute a significant threat to agriculture, resulting in annual crop yield reductions estimated at $100 billion (Bernard et al., 2017). Among these, the most detrimental are sedentary endoparasitic nematodes, particularly cyst (*Globodera* and *Heterodera spp*.) and root knot nematodes (*Meloidogyne spp*.) (Tapia-Vázquez et al., 2022). Root knot nematodes induce localised swelling in their host plants, resulting in the formation of galls. Inside galls, nematodes multiply and obtain nutrients from the plant's vascular tissues, substantially affecting plant growth, development, and yield (Ravindra et al., 2017).

Although extracts from various agricultural byproducts have been utilised to enhance plant resistance against a range of pests, this study is the first to evaluate the bioprotectant potential of fruit peel extracts from the genus *Prunus* (Rosaceae) against *Meloidogyne graminicola* (Mg), a root knot nematode that can cause yield losses ranging from 5 to 73 % in aerobic rice cultivation systems (Mantelin et al., 2016; Kumar et al., 2020). Considering that rice is the staple food for approximately half of the world's population and plays a crucial role in global food security (FAO 2021), mitigating the impact of Mg is of significant importance. The threat from Mg is expected to rise as traditional flooded rice cultivation, which is environmentally challenging owing to high freshwater consumption and methane emissions, is progressively being replaced by aerobic rice systems (Gupta et al., 2021; Mahapatra et al., 2021). Although these water efficient and eco-friendly systems offer several advantages, they are, unfortunately, more susceptible to Mg infestation (Yang et al., 2023).

Rosaceae fruit byproducts, such as peach, plum, and apricot peels, are rich in bioactive compounds. These include flavonoids (rutin, naringenin, quercetin), polyphenols (chlorogenic acid, catechin), and triterpenoids, all shown to have antimicrobial and nematicidal potential (Gedük and Atsız 2022; Liu et al., 2015). Rutin primes salicylic acid-dependent defences in rice (Yang et al., 2016), while naringenin activates immune signaling in Arabidopsis (An et al., 2021). Thus, Rosaceae byproducts offer promising, sustainable sources of bioprotectants.

This study investigates aqueous peel extracts from peach (*Prunus persica*, PPE), apricot (*Prunus armeniaca*, APE), and plum *(Prunus domestica*, PLPE) as potential bioprotectants against Meloidogyne graminicola in rice. We reveal the dual action of PPE through direct nematicidal activity and induced resistance and provide mechanistic insights into the pathways activated inside treated rice plants.

2. Materials and methods

2.1. Rice seed germination

The seeds of *Oryza sativa* cv. 'Nipponbare' (rice) seeds were germinated at 30 °C for four days. Following germination, the seedlings were placed in substrate inside cylindrical PVC tubes. The tubes, measuring 18 cm in length and 3 cm in diameter, were equipped with a mesh covered base to enable water drainage. A substrate comprising sand and the absorbent polymer AquaPerla® (Belgium) was used. The tubes containing germinated seedlings were maintained at 28 °C in a controlled rice growth chamber with a photoperiod of 12 h light at 150 μmol/m^2/s, followed by 12 h of darkness in a 24-hour cycle. The relative humidity was maintained at 70–75 %. Nutrients essential for optimal rice plant growth were supplied via 10 ml of Hoagland's solution thrice a week (Hoagland 1920).

2.2. Extract preparation and treatment

Fruits were purchased from a local supermarket in Ghent, Belgium. The samples were then washed to remove dust and foreign particles. After washing, the fruit was dried and peeled. To prepare the peel extracts, 300 g of peel was blended with 1000 mL of distilled water. The blended mixture was maintained overnight at 4 °C and filtered through a Whatman No 1 filter paper. The extracts were then centrifuged for 8–10 min at 5000 rpm to eliminate suspended particles. The resulting extracts were stored at −20 °C until further use.

Two-week-old plants were treated with extracts formulated using 0.02 % (v/v) Tween20 as a surfactant. Five mL of the extract were sprayed onto 10 plants for each treatment. Mock treated plants were sprayed with water containing 0.02 % Tween20. After two weeks, plant shoot and root lengths were measured. Plants were also observed for any signs of chlorosis or necrosis caused by the treatment.

2.3. Root knot nematode infection experiment

Barnyard grass (*Echinochloa crus-galli*) was used to maintain a pure culture of the root knot nematode *Meloidogyne graminicola*. A modified Baermann funnel method was employed to extract second stage nematode juveniles from the roots of barnyard grass (Whitehead and Hemming 1965). Rice plants were cultivated in SAP media for two weeks and subsequently treated with the extracts. One day post treatment, the rice roots were inoculated with 250 second stage Mg juveniles (J2). Plant susceptibility to Mg was evaluated 14 days post inoculation by quantifying the total number of nematodes, galls, and egg producing females. This was performed using the acid fuchsin staining technique (Bybd Jr, Kirkpatrick et al., 1983). The galls and nematodes were counted using a binocular Leica stereomicroscope. All infection experiments included 10 plants per treatment. Dehydroascorbic acid (DHA; 20 mM) was used as positive control and distilled water with 0.02 % Tween 20 was used as a mock treatment (Chavan et al., 2022). One of the infection experiments was conducted on JA deficient mutant 'Hebiba' (Riemann et al., 2003) plants and their wild type Nihonmasari under the same experimental conditions as described above.

2.4. Nematicidal assay

An experiment was conducted to evaluate the nematicidal efficacy of the extracts against J2 stage Mg root knot nematodes. The experiments were performed in 12 well plates, with each well containing approximately 100 J2 nematodes suspended in 2 mL of 50 % extract solution. Sterilised tap water was used as a negative control. The treatments were replicated three times. Following a 24-hour incubation period, observations were made using a stereomicroscope.

2.5. DAB assay for histochemical H_2O_2 detection

DAB (3, 3-diaminobenzidine) was used to analyse H_2O_2 accumulation in treated rice leaves following a protocol by Daudi and O'brien (2012). Rice plant leaves were subjected to treatment by applying 10 μL droplets of extracts and using distilled water with 0.02% Tween20 as a control treatment. The treated leaf sections were sampled at 6, 12, and

24 hours post treatment (hpt). These sections were subsequently vacuum infiltrated (60KPa) in DAB solution (1 mg/mL) for 5 min and then incubated in the dark for 4 h. The DAB treated leaves were bleached in a hot water bath for 15 min at 95°C using a solution of acetic acid, glycerol, and ethanol at a ratio of 1:1:3 (v:v:v). The polymerisation products of H_2O_2 were visualised as deep brown spots using a Leica stereomicroscope.

2.6. Spatial temporal dynamics of the ROS burst

ROS dynamics in treated leaves was monitored using non-destructive imaging with a fluorescent probe, 2′,7′-dichlorodihydrofluorescein diacetate (H_2DCFDA), following the protocol described by Kaur, Sharma et al., (2016) with slight modifications. The rice plants were grown hydroponically in 50 % Hoagland's solution for two weeks under the same environmental conditions as described in section 2.1. The upper 1 cm of the leaves were sprayed with PPE formulated with 0.02 % Tween 20. Subsequently, the entire plant was infiltrated with H_2DCFDA at a concentration of 10 μM under a vacuum of 60 kPa for 5 min. Plants were handled cautiously to prevent bending or folding of the leaves or roots, which may cause a false positive ROS signal. Following infiltration with the fluorescent probe, the leaves were rinsed twice with distilled water. Subsequently, a confocal microscope (Nikon A1R) was used to observe ROS induced fluorescence. The samples were visualised at a 485/535 nm (Ex/Em) wavelength, and the Nikon NIS Elements software package was used for image acquisition. Images were processed using the ImageJ software. A total of 17 images were taken for each point of interest at 15 min intervals, starting from 0.5 hpt up to 4.5 hpt. The average intensity of five Z-stacks was used at each time point to account for the different fluorescence intensities at different leaf depths.

2.7. Biochemical assays

For each biochemical assay, six biological and three technical replicates were used. The plant samples were thoroughly washed with water to remove the residual substrate. After cleaning, the plant tissues were snap frozen in liquid nitrogen, finely ground, and stored at −80 °C until further use.

2.7.1. H_2O_2 quantification

Hydrogen peroxide levels in plant samples were measured using a modified ferrous oxidation xylenol orange (FOX) assay method. Approximately 100 mg of plant material was ground in 1 mL of 2.5 % trichloroacetic acid and centrifuged at 13,000 rpm for 9 min at 4 °C to isolate the supernatant. The FOX reagent consisted of two components: reagent A (125 μM xylenol orange, 1 % ethanol, 100 mM sorbitol) and reagent B (25 mM ferrous ammonium sulfate, 2.5 M sulfuric acid), mixed in a 100:1 ratio immediately before use. For measurement, 0.2 mL of supernatant was combined with 1 mL of freshly prepared FOX reagent, vortexed thoroughly, and incubated in the dark at 25 °C for 30 min. Triplicate absorbance readings were recorded at 595 nm using a spectrophotometer. The final H_2O_2 concentrations were calculated using a reference curve developed from standard hydrogen peroxide solutions (De Kock et al., 2024).

2.7.2. MDA quantification

To quantify malondialdehyde (MDA) levels, fresh reagent preparations were prioritised owing to their limited stability. Two solutions were prepared: RSI (150 μL of butylated hydroxytoluene (BHT) was mixed with 30 mL of 20 % trichloroacetic acid (TCA)) and heated to 70 °C until fully dissolved, and RSII (0.195 g of thiobarbituric acid (TBA)) dissolved in 30 mL of RSI under identical heating conditions. Plant tissue (100 mg) was homogenised in 1 mL of 0.5 % TCA, centrifuged at 13,000 rpm (4 °C, 15 min), and split into two 250 μL aliquots. Each aliquot was mixed with 250 μL of either RSI or RSII and heated to 95 °C for 30 min. The reactions were stopped by rapid cooling on ice. Absorbance was measured at 440 nm, 532 nm, and 600 nm using a Tecan 96-well plate reader. MDA concentration (nmol mL^{-1} g^{-1}) was derived using the following equation, which accounts for nonspecific absorbance at 600 nm to isolate MDA-TBA adduct signals (Hodges et al., 1999)

$$A = (\mathrm{Abs532}_{\mathrm{RS\ II}} - \mathrm{Abs600}_{\mathrm{RS\ II}}) - (\mathrm{Abs532}_{\mathrm{RS\ I}} - \mathrm{Abs600}_{\mathrm{RS\ I}})$$

$$B = (\mathrm{Abs440}_{\mathrm{RS\ II}} - \mathrm{Abs600}_{\mathrm{RS\ II}}) \times 0.0571$$

$$\mathrm{MDA} = \left(\frac{A - B}{157\ 000}\right) \times \frac{1000\ 000}{\textit{fresh sample weight}\ (g)}$$

2.7.3. Total phenolic and flavonoid content

The total phenolic content in the treated rice plants was quantified using a modified Folin Ciocalteu method (Nikolaeva et al., 2022). Dried plant samples were homogenised and extracted with 95 % methanol (1:10, w/v) for 12 h. For analysis, 15 μL of extract was reacted with 75 μL of 10 % v/v Folin Ciocalteu reagent and 70 μL of 10 % w/v Na_2CO_3 in a 96-well plate. A gallic acid calibration curve (0–100 μg/mL) was established with water serving as the blank. After 30 min of incubation in the dark at 25 °C, the absorbance was measured at 765 nm. The results were expressed as gallic acid equivalents (GE) per gram of dry weight.

The total flavonoid content was determined using aluminium chloride (Shraim et al., 2021). A reaction mixture containing 21 μL extract, 85 μL methanol, 21 μL 1 M CH_3COONa, and 21 μL 2 % $AlCl_3$ was incubated for 30 min. Absorbance at 430 nm was compared against a quercetin standard curve, and the results were expressed as quercetin equivalents (QE) per gram dry weight. All spectrophotometric measurements were performed in triplicates using a Tecan 96-well plate reader.

2.8. Transcriptome analysis

Transcriptome profiling using RNAseq was executed to evaluate genome-wide expression changes in rice plants at 2 time points after PPE treatment. Two-week-old rice plants were sprayed with PPE solution containing 0.02 % Tween20, the whole plant sample was collected at 6 and 24 h post application. The control groups received mock treatments (water with 0.02 % Tween20) and were sampled identically. The study design incorporated three biological replicates per condition, each containing pooled tissue from four plants. Total RNA was purified using the RNeasy Plant Mini Kit and its quality was verified using an Agilent 2100 Bioanalyzer. High integrity RNA (1 μg) was processed with the QuantSeq 3′ mRNA Seq Kit to generate strand specific libraries, followed by size selection on 2 % ultra-agarose gels. Multiplexed libraries were denatured, diluted to 6 pM, and sequenced on an Illumina NextSeq 500 platform (75-cycle single end reads).

The raw sequencing data were subjected to adapter trimming and quality filtering. Transcript quantification was performed using Salmon's quasi mapping algorithm against the Rice Annotation Project Database (v38) (Patrol et al., 2017). Differential expression was analyzed via DESeq2 (FDR-adjusted $p < 0.05$) (Lawrence et al., 2013), while the enriched biological pathways were determined through ShinyGO (Ge et al., 2020). All sequence files were archived under NCBI BioProject PRJNA1204074.

2.9. Hormone measurements

Phytohormone profiling of PPE treated rice plants was conducted using targeted ultra-high performance liquid chromatography coupled with high resolution mass spectrometry (UHPLC—HRMS). Root and shoot tissues from two-week-old plants at 24 hpt were extracted using a chilled modified Bieleski solvent system followed by centrifugation-based purification. Six biological replicates per treatment group, each comprising pooled samples from three individual plants, were analysed for indole-3-acetic acid, salicylic acid, abscisic acid, and jasmonic acid

concentrations. Analytical separation and quantification were achieved using the Orbitrap based Q-Exactive™ platform (Haeck et al., 2018).

2.10. LC-MS analyses for untargeted metabolomics

LC-MS analysis was carried out to identify the bioactive compounds present in PPE and to analyse the metabolomic changes in rice shoots and roots upon treatment with PPE in and untargeted metabolomic experiment. The raw untargeted metabolomics data generated in this study are available in the MassIVE repository under the dataset identifier MSV000099534.

2.10.1. Compound identification in PPE

Peach peels were thoroughly washed, air dried, and finely ground to increase extraction efficiency. The ground peels were then sonicated for 30 min in 70 % methanol at a solvent to sample ratio of 10:1 (mL/g). The methanolic extract was centrifuged at 8000 rpm for 10 min to remove any solid residue. To ensure sample purity and prevent instrument contamination, each extract was further purified by filtration through a 0.22 μm PTFE syringe driven filter. The filtered extract (500 μL) was diluted to 1000 μL for LC-MS Orbitrap analysis. A 50 μL sample was injected into the HPLC system for analysis.

The analytical workflow utilised an Agilent 1260 Infinity II high performance liquid chromatography (HPLC) system coupled with a Thermo Scientific Q Exactive HF-X Hybrid Quadrupole Orbitrap mass spectrometer. The HPLC system was configured with an auto sampler, thermostatted column compartment, and quaternary pump. Chromatographic separation was performed using a Macherey-Nagel™ Gravity analytical column (3.0 × 100 mm, 1.8 μm particle size). The mobile phase consisted of two components: (A) 0.1 % formic acid in water (B) and 0.1 % formic acid in methanol. A linear gradient elution method was employed, starting with 10 % B and increasing to 90 % B over 6.5 min. This ratio was held for 1.5 min before returning to 10 % B for 1.0 min, with a 1 min equilibration interval before and after each run (Shah, Ramzan et al., 2023).

LC-MS data were acquired using an HPLC Orbitrap system in negative ionisation mode with Data Dependent Acquisition (DDA) over a 0.3–15 min retention time window and subsequently processed using MZmine 4.6.1. The MZwizard function facilitated the initial workflow setup tailored for Orbitrap DDA data, and batch processing was employed for efficient analysis of multiple samples, including blank and QC samples. The processing pipeline involved raw data import, mass detection (MS1/MS2), chromatogram building, deconvolution, feature filtering, isotopic peak grouping, feature alignment across samples using optimised *m/z* and RT tolerances, and gap filling. Publicly available databases in MZmine, such as GNPS, were utilised for the annotation of spectra using accurate mass and retention times, with confidence levels assigned to all annotations based on the available evidence (Schmid, Heuckeroth et al., 2023).

2.10.2. Untargeted metabolomic analysis of PPE treated rice plants

An untargeted metabolomics approach was used to profile metabolic changes in an unbiased way, both in locally treated tissue (leaves) and systemically (roots). Two-week-old rice plants (*Oryza sativa*) were sprayed with PPE solution containing 0.02 % Tween20, and tissue was collected at 24 h post application. Leaf and root tissue was separately sampled and immediately snap frozen in liquid nitrogen, ground to a fine powder, and stored at −80 °C. Metabolites were extracted and quantified as detailed in Section 2.10.1.

For LC-MS analysis, vendor raw files were converted to mzML format using MSConvert (ProteoWizard) and subsequently processed using MS-DIAL software. Data processing was performed in **negative ion mode** with a retention time window of 0.5 to 15 min and a mass-to-charge ratio (*m/z*) range of 70–1050. Peak detection parameters included a minimum intensity threshold of 10,000 arbitrary units (a.u.), a mass slice width of 0.1 Da, linear weighted smoothing applied across two consecutive scans, and a minimum peak width requirement of five scans. Spectral deconvolution of co-eluting compounds was performed using MS2Dec with the following parameters: sigma (σ) = 0.5, minimum abundance threshold ≥ 10 a.u., and precursor exclusion enabled. Feature annotation was conducted by matching against public MSP spectral libraries in negative ion mode, applying mass tolerances of 0.01 Da for MS^1 and 0.05 Da for MS^2 spectra. Sample alignment was performed using a pooled quality control (QC) reference with retention time tolerance of ±0.05 min and mass tolerance of ±0.025 Da. Features were retained if present in ≥25 % of all sample injections or in ≥16.7 % of samples within any treatment group. Missing values in the resulting data matrix were addressed through algorithmic gap-filling procedures. Signals detected in procedural blanks were removed. The resulting peak area matrix was subjected to Student's *t*-tests, yielding p-values and $\log_2$ fold changes. Differential metabolites were visualised on a volcano plot, with the most significant compounds annotated (Takeda et al., 2024).

2.11. Statistical analysis

Quantitative comparisons between the experimental groups were performed using parametric statistical methods. Normality assumptions were first verified through appropriate diagnostic checks, followed by the implementation of one-way or two-way ANOVA, with subsequent post hoc comparisons against mock treated controls as baseline comparators. All analyses maintained a significance threshold of α=0.05, with graphical outputs displayed as asterisks ($*p < 0.05$, $**p < 0.01$, $***p < 0.001$) to mark significant deviations from the control values. Data processing and visualisation were performed using GraphPad Prism 9.3. software to ensure analytical rigor in evaluating treatment induced physiological responses.

3. Results

3.1. Peach peeling extract acts as a bioprotectant against nematodes in rice while showing no phytotoxic effects

Based on previous research we hypothesized that Rosaceae peeling extracts would contain bioactive compounds that could induce systemic resistance or act nematicidal. After preparation of peach, apricot, and plum peeling extracts (PPE, APE, and PLPE, respectively), they were evaluated for phytotoxicity upon foliar application in rice plants, and the results indicated no negative effects on any of the investigated parameters (Fig. S1). To assess the induction of systemic resistance in rice plants by PPE, APE, and PLPE, an infection experiment with root knot nematode *M. graminicola* (Mg) was conducted. Foliar spray treatment was selected to prevent direct contact between the extracts and nematodes and was performed one day before root inoculation. Treatment with PPE, but not with APE and PLPE, resulted in a significant reduction in the number of galls, total number of nematodes, and egg laying females compared to the mock treated control (Fig. 1a).

3.2. Direct nematicidal activity of PPE, APE, and PLPE

In addition to the infection experiment, nematicidal assays were performed to assess the direct effects of PPE, APE, and PLPE on nematodes. All three extracts demonstrated significant nematicidal potential, resulting in nematode mortality upon direct contact. The PPE extract exhibited the highest mortality rate (92 %), followed by APE (66 %) and PLPE (45 %), normalised against the mock treated control group (Fig. 1b). The extracts were also screened for pesticide contaminants, which could have caused biological effects; however, no significant pesticide contaminants were detected (Table S1).

3.3. PPE induces a ROS burst in rice leaves

The accumulation of ROS, such as H_2O_2, is a hallmark of induced

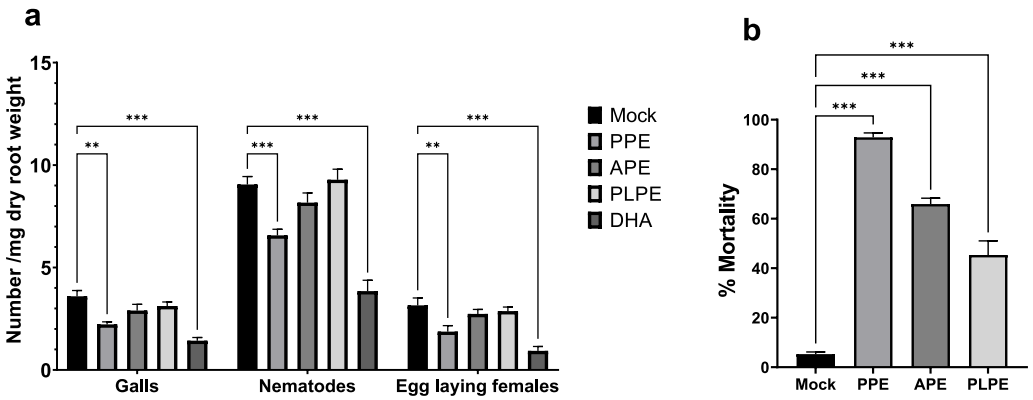

Fig. 1. (a) Effect of PPE, APE, and PLPE foliar spray treatment on Meloidogyne graminicola number of galls, total number of nematodes, and egg-laying females in rice roots. (b) For nematicidal activity, the results are expressed as percentage mortality normalised against the mock control. A two-way ANOVA for the infection experiment and one-way ANOVA for the nematicidal assay followed by Dunnett's multiple comparison test was performed with Mock as the control group at $\alpha = 0.05$. Error bars representing standard error of mean and asterisks on error bars indicate statistically significant differences between the mock and treated plants (*$p < 0.05$, **$p < 0.01$, ***$p < 0.001$). DHA: dehydroascorbic acid.

resistance (O'Brien et al., 2012). For the initial screening of H_2O_2 accumulation in extract treated rice leaves, 3,3′-diaminobenzidine (DAB) staining was used. This method is useful for assessing the localised accumulation of H_2O_2 in plant leaves (Chavan, De Kesel et al., 2022) DAB staining was conducted at three time points: 6, 12, and 24 hpt with PPE. DAB staining was noticeably pronounced in the areas where the extracts were applied (Fig. 2a). At 6 hpt, rice leaves treated with PPE and APE exhibited slight H_2O_2 accumulation, as evidenced by faint brown staining, whereas leaves treated with PLPE showed no staining. At 12 hpt, increased staining intensity was observed in leaves treated with PPE and APE, indicating elevated H_2O_2 levels, whereas PLPE treated plants were slightly stained. At 24 hpt, significant staining was evident in leaves treated with all three extracts (Fig. 2a).

Following qualitative assessment with DAB staining, quantitative analyses of H_2O_2 and MDA levels were conducted at 12 and 24 hpt for the whole plant. PPE treatment resulted in a significant increase in both H_2O_2 and MDA concentrations compared to the mock treated control, indicating increased ROS production and lipid peroxidation (Fig. 2b&c). In contrast, treatments with APE and PLPE did not show any significant differences in H_2O_2 and MDA levels relative to the control. A transient

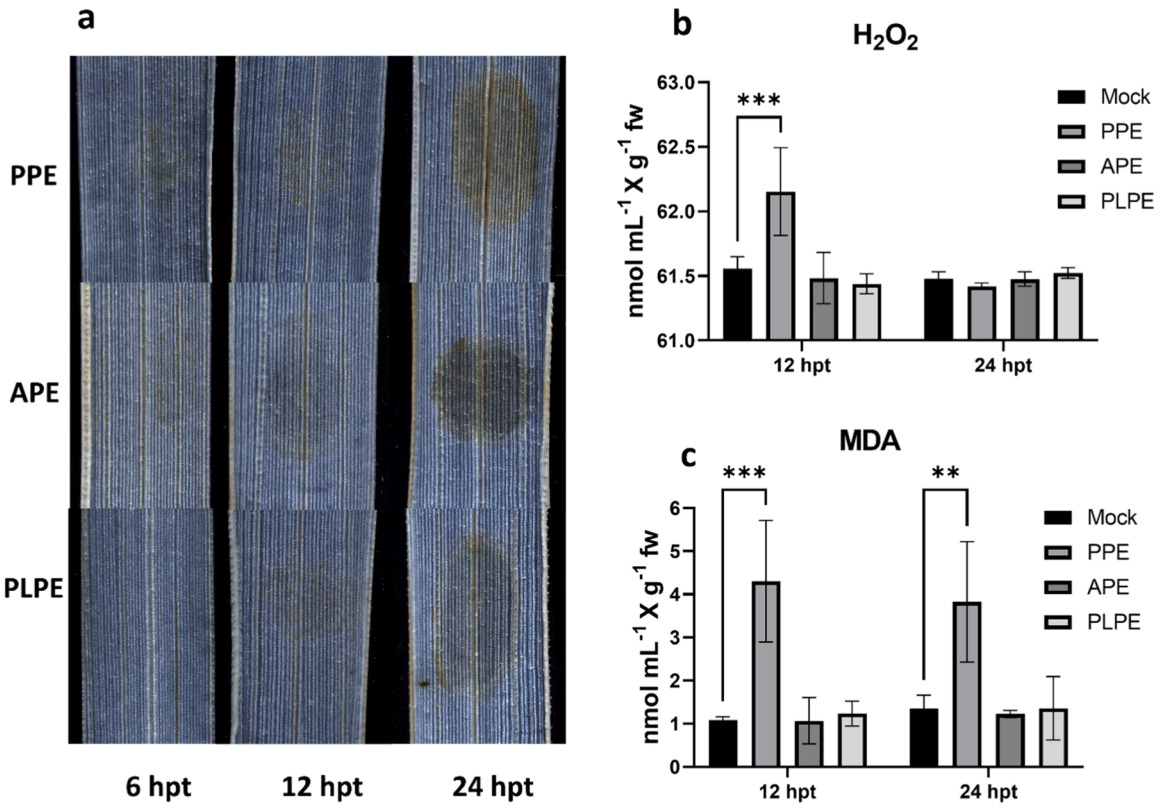

Fig. 2. ROS response in treated rice leaves. (a) DAB staining shows H_2O_2 accumulation in rice leaves treated with PPE, APE and PLPE at 6,12 and 24 hpt. (b) represents H_2O_2 concentrations expressed in nanomoles per gram of plant fresh weight at 12 hpt and 24 hpt, and (c) represents MDA concentrations expressed in nanomoles per gram of plant fresh weight at 12 hpt and 24 hpt. A two-way ANOVA followed by Dunnett's multiple comparison test was conducted with the Mock group as the control at $\alpha = 0.05$. Error bars representing standard error of mean and asterisks on error bars indicate statistically significant differences between the mock and treated plants (*$p < 0.05$, **$p < 0.01$, ***$p < 0.001$).

peak of H_2O_2 accumulation was observed at 12 hpt, whereas the MDA concentration remained significantly higher at both 12 and 24 hpt in PPE treated plants than in the mock treatment.

As these initial results support ROS accumulation due to PPE treatment, we further evaluated local ROS dynamics in a non-destructive imaging assay using the H_2DCFDA fluorescence probe, which reflects the presence of various ROS, including hydrogen peroxide (H_2O_2), superoxide anions ($O_2^{\bullet-}$), and hydroxyl radicals (•OH). Fluorescence intensity measurements were taken at 15-min intervals, starting 30 min after the treatment and continuing for 4.5 h (Fig. 3a). The upper 1 cm of the rice leaf was treated with PPE, and measurements were taken 1 cm (point A) below the point of treatment (POT) and 3 cm (point B) from the POT, as shown in Fig. 3b The initial measurement at 0.5 hpt shows an identical background ROS at both points. Over time, the ROS at these points increased, with the peak intensity observed at 2.2 hpt at point A and 3.0 hpt at point B. The maximum ROS accumulation at point A was slightly higher, and it increased more rapidly than that at point B. However, the ROS response at point B, while less intense, persisted for a longer period (Fig. 3). This experiment demonstrated a systemic and time dependent spread of ROS in rice leaves treated with PPE.

3.4. PPE induced resistance is dependent on the jasmonate pathway

Given the significant results of PPE in infection and biochemical assays, we further explored the molecular mechanisms underlying PPE induced systemic resistance in rice plants at two time points: 6 hpt and 24 hpt. To gain insight into the early and late transcriptional responses to PPE, we performed RNA Seq on the PPE treated rice plants.

At 6 hpt, particularly genes associated with JA signalling (*OsJAmyb, OsJAZ1, OsLOX11*), secondary metabolite biosynthesis, such as flavonoids and terpenes (*OsF3H-2, OsFLS, OsTPS3, OsTPS31, OsTPS*), ROS signalling (*OsPOX8.1, OsPOX22.3*), and other defence related genes linked to IR, including *OsWRKY45, OsICE1*, and *OsNPR3*, were differentially expressed (Fig. 4a).

At 24 hpt, PPE treatment induced significant changes in the expression of genes involved in ROS regulation (*OsGSTU26, OsGSTU12,* and *OsGRX6*), JA signalling (*OsJMT-2, OsJAC1,* and *OsJAZ4*), secondary metabolite biosynthesis (*OsTPS31, OsTPS3, OsFLS,* and *OsTPS*), and plant defence regulation (transcription factors *OsWRKY71* and *OsWRKY53*) (Fig. 4b).

Gene Ontology (GO) enrichment analysis of Biological Processes was performed on DEGs at both time points (Fig. 4c). At 6 hpt, GO terms associated with upregulated DEGs indicated plant defence responses, including JA mediated signalling pathways, aromatic amino acid family biosynthetic processes, cellular responses to JA and fatty acids, phenylpropanoid metabolic processes, and responses to ROS and chemical stimuli (**Table S2**). Downregulated DEGs at 6 hpt were primarily associated with thiamine biosynthesis and metabolic processes, primary alcohol biosynthesis, and cytokinin activated signalling pathways (**Table S3**). GO enrichment analysis of the 24 hpt DEGs revealed similar enrichment patterns, with upregulated DEGs associated with the regulation of JA mediated signalling pathways, responses to wounding,

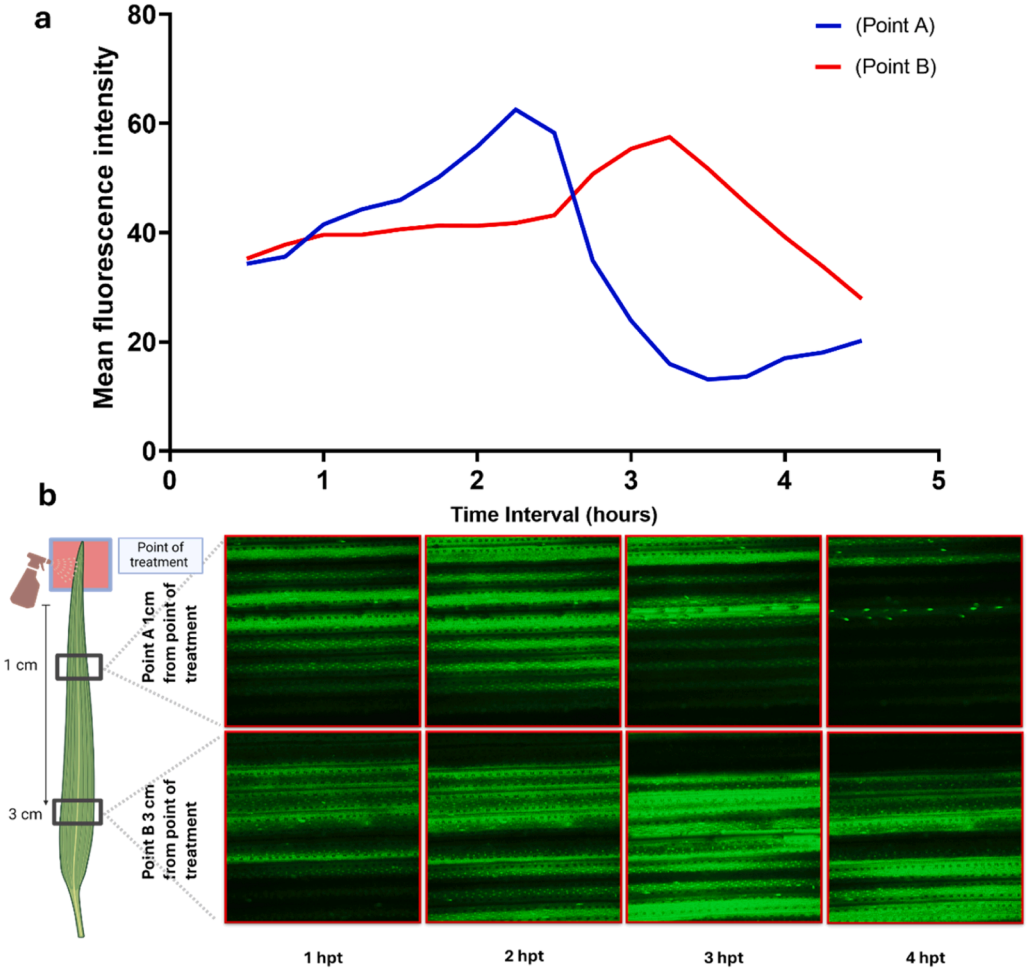

Fig. 3. ROS visualization with H_2DCFDA (a) quantitative data for point A (1 cm away from the point of treatment with PPE) and point B (3 cm away from the point of treatment with PPE). (b) ROS-induced fluorescence in rice leaves treated with PPE. Images represent the fluorescence intensity at 1, 2, 3, and 4 hpt for both point A and point B normalized against mock treatment.

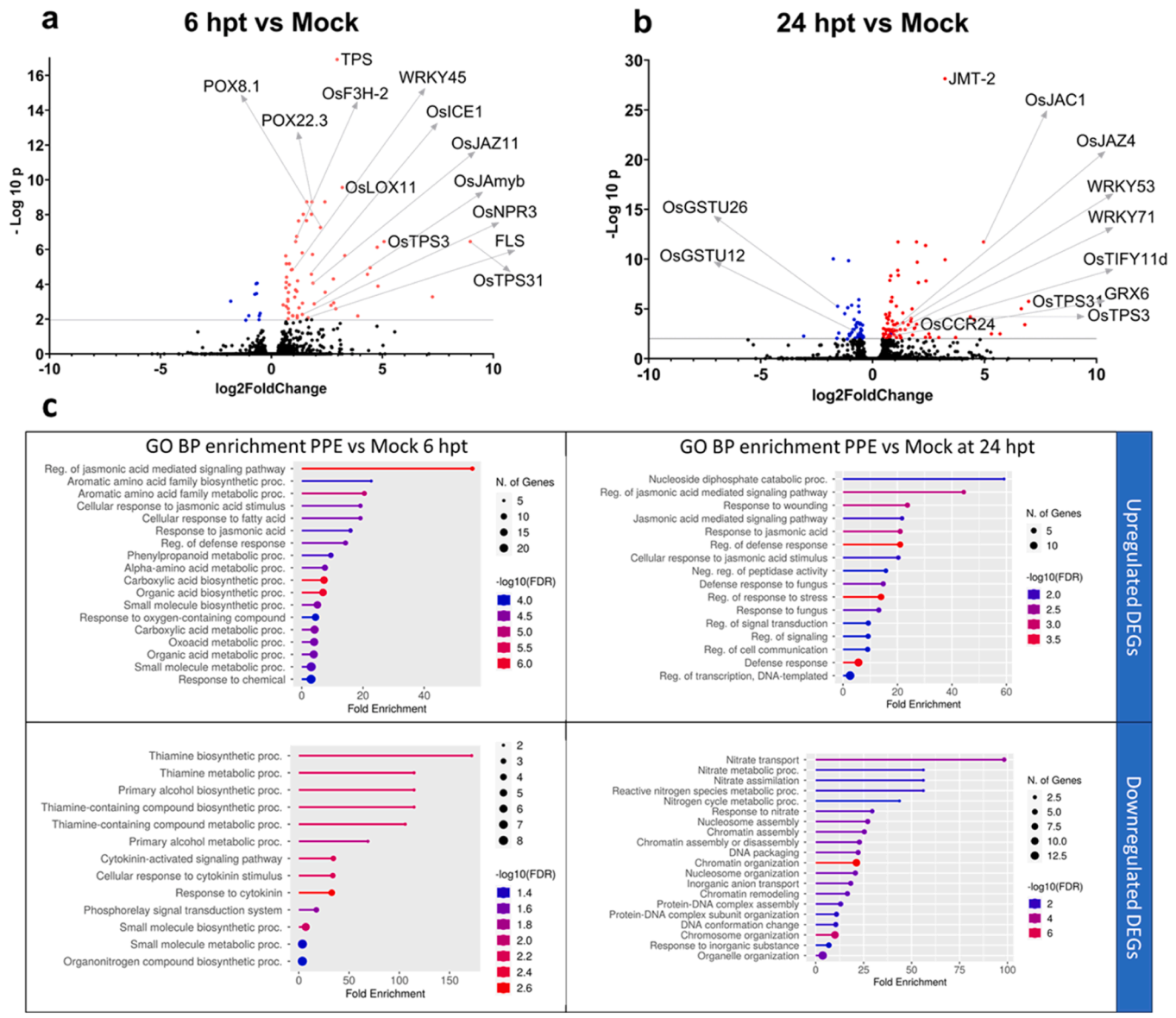

Fig. 4. Transcriptomic response of rice plants to PPE treatment at 6 and 24 hpt. Fig a & b volcano plots showing differentially expressed genes (DEGs) at 6 hpt (a) and 24 hpt (b) compared to mock-treated controls. Red and blue dots represent significantly upregulated and downregulated genes, respectively. Statistical significance in transcriptome analyses was determined using the Benjamini-Hochberg method to control the false discovery rate with FDR < 0.05. Fig c Gene Ontology enrichment analysis of biological processes associated with DEGs. Top panels show enriched terms among upregulated genes; bottom panels show those among downregulated genes.

defence responses to fungi, and overall stress responses (**Table S4)**. A notable difference between 24 hpt and 6 hpt was the significant enrichment of GO terms related to nucleoside diphosphate catabolic processes at 24 hpt, indicating active nucleotide metabolism. The downregulated DEGs at 24 hpt were associated with nitrate transport, metabolic processes, chromosomal reorganisation, nucleosome and chromatin assembly, and protein DNA complex assembly, highlighting significant changes in genomic reorganisation and nitrogen metabolism (**Table S5**).

Transcriptomic profiling revealed substantial activation of DEGs linked to phytohormone pathways in rice plants exposed to PPE treatment. Quantitative analysis of JA, IAA, ABA, and SA levels at 24 hpt (Fig. 5) showed that roots of PPE treated plants exhibited a 1.5 fold increase in JA concentration while a more than 2-fold increase in ABA levels was observed in shoot tissues compared to mock treated plants. The treated rice plants did not show any significant changes in IAA and SA levels compared with the mock treatment. To confirm the functional involvement of JA in PPE induced resistance, comparative infection studies were conducted using the JA biosynthesis 'Hebiba' mutant and its wild-type counterpart, Nihonmasari (Fig. 5e). Wild type plants treated with PPE showed more than a 50 % reduction in both gall formation and nematode counts compared to untreated controls, consistent with prior observations in the Nipponbare cultivar. In contrast, PPE application caused no measurable decrease in nematode infection rates in the JA deficient 'Hebiba' mutant, indicating that an intact JA pathway is essential for the IR effects of PPE treatment.

3.5. PPE induces local accumulation of total phenolic and flavonoid content

Total phenolic and flavonoid contents were quantified separately in shoots and roots following foliar application of PPE, APE, PLPE, or mock. In shoots, PPE increased total phenolics by 39 % and total flavonoids by 31 % relative to mock (Fig. 6a, b), whereas APE and PLPE did

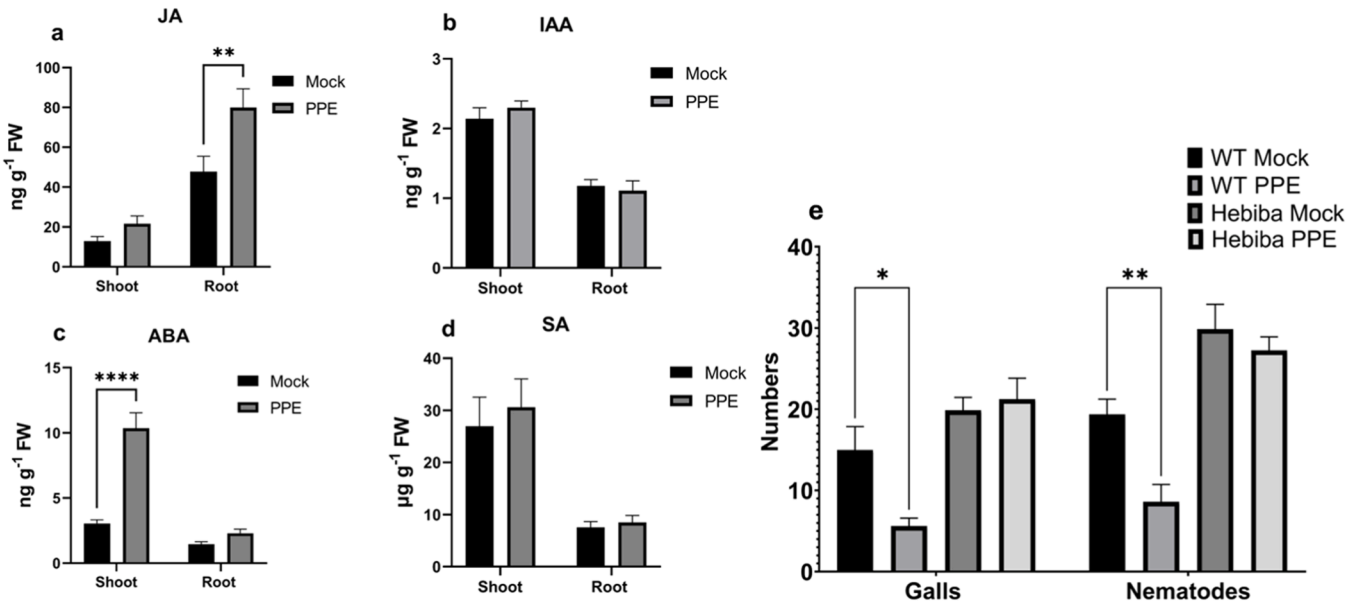

Fig. 5. Hormonal responses and infection outcomes in PPE-treated rice plants at 24 hpt with quantification of hormone levels in shoots and roots. Measured hormones (a) jasmonic acid (JA), (b) indole-3-acetic acid (IAA), (c) abscisic acid (ABA), and (d) salicylic acid (SA). (e) Infection assay in the JA biosynthesis mutant line Oryza sativa Hebiba and wild type (WT). The number of galls and nematodes was quantified to assess susceptibility. Statistical analysis was performed with significance relative to Mock. Data were analyzed using two-way ANOVA followed by Dunnett's multiple comparison test with the mock group as control ($\alpha = 0.05$). Error bars represent standard error of the mean, asterisks indicate statistically significant differences (*$p < 0.05$, **$p < 0.01$, ***$p < 0.001$, ****$p < 0.0001$).

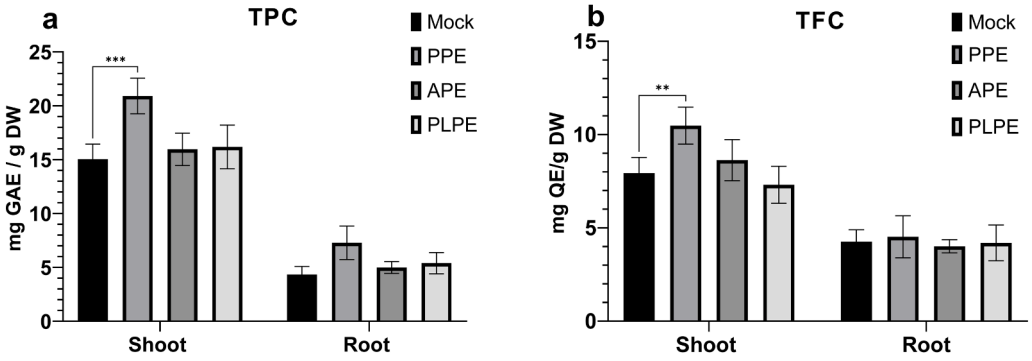

Fig. 6. Effect of PPE, APE and PLPE treatment on rice total phenolic and flavonoid content. (a) represents the total phenolic content (TPC) in gallic acid equivalents, and subfigure (b) represents the total flavonoid content (TFC) in quercetin equivalents, in both the shoots and roots of rice plants 24 hpt. A two-way ANOVA followed by Dunnett's multiple comparison test was conducted with the Mock group as the control at $\alpha = 0.05$. Error bars representing standard error of mean and asterisks on error bars indicate statistically significant differences between the mock and treated plants (*$p < 0.05$, **$p < 0.01$, ***$p < 0.001$).

not cause significant changes. In roots, total phenolic and flavonoid levels did not differ significantly between PPE and mock at the sampled time points. These assays were complemented with untargeted LC–MS, which has the potential to reveal differential accumulation of specific defence-related metabolites.

3.6. Metabolomics on treated rice plants shows systemic accumulation of specific phenylpropanoid derived compounds upon PPE treatment

Untargeted screening of metabolites in PPE treated rice plants at 24 hpt revealed an array of metabolomic changes in both roots and shoots, as shown in Fig 7. The accumulation of several key metabolites demonstrated the plant's enhanced defence response i.e. the accumulation of 1-methylsulfinylbutenyl isothiocyanate, a glucosinolate derived compound that is hydrolysed by myrosinase upon tissue damage to form isothiocyanates with potent antimicrobial and nematicidal properties (Eugui et al., 2022). The analysis also revealed elevated levels of resveratrol, a well-known phytoalexin (stilbene) produced under plant stress conditions. Both trans-resveratrol and its dimers, which accumulate upon fungal infection or wounding, demonstrate significant antimicrobial activity and can effectively inhibit pathogen growth (Song et al., 2021). Furthermore, colneleic acid, an oxylipin (divinyl ether fatty acid) produced through the 9-LOX pathway during pathogen attack, was detected. This compound accumulates in infected tissues of potato and tobacco, directly inhibiting oomycetes and fungi, while in tomato, it accumulates in roots during *Meloidogyne javanica* infection and reduces infection severity. The phenylpropanoid pathway was also highly active, as evidenced by the abundance of caffeic acid, a phenolic intermediate with antioxidant and antimicrobial properties that serves as a direct precursor for lignin synthesis. Similarly, sinapyl alcohol, a syringyl lignin monomer that polymerizes into lignin to strengthen cell walls, was found in abundant quantities. Overall, the abundance of defence related metabolites in shoots indicates a robust defence response in PPE treated rice plants.

In the root tissue, we detected accumulation of compounds like caffeic acid, quercetin glycoside, azelaic acid, and galloylglucose that could enhance plant immunity by boosting antioxidant capacity, reinforcing cell walls, and providing antimicrobial activity. Elevated levels

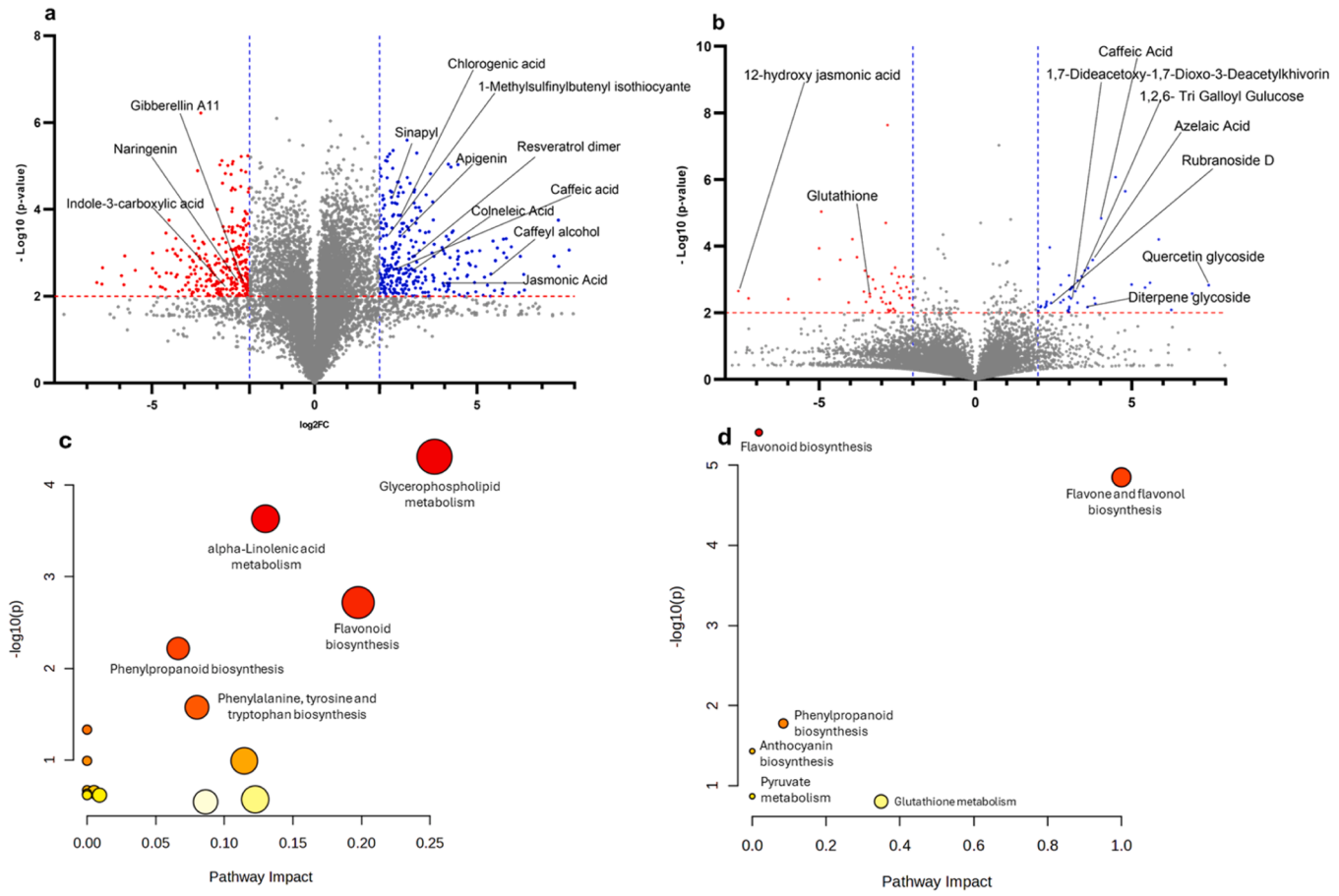

Fig. 7. Untargeted metabolomic profiling of PPE-treated rice plants at 24 hpt. Volcano plots showing significantly altered metabolites in shoot (a) and root (b) samples. Statistical significance was calculated using false discovery rate, with FDR < 0.05. Metabolites with high fold changes and statistical significance are highlighted in blue are significantly higher abandoned and red are significantly less abundant compared to mock treated plants. The bubble plot illustrates the KEEG pathway enrichment of significant metabolites in shoot (c) and root (d).

of diterpene and limonoid glycosides suggest activation of phytoalexin based defences. Meanwhile, lower levels of 12-hydroxy jasmonic acid may indicate the sustained JA signalling (Miersch, Neumerkel et al., 2008), and decreased glutathione likely reflects activation of ROS signalling.

A KEGG enrichment analysis of shoot and root metabolites (Fig. 7c & d) reveals a coordinated metabolic response underlying systemic IR. In shoots, pathways like glycerophospholipid metabolism and alpha linolenic acid metabolism are highly enriched, highlighting the importance of lipid signalling and jasmonic acid biosynthesis in initiating systemic defence. In roots, flavonoid biosynthesis is again prominent, along with flavone/flavonol biosynthesis, indicating a strong antioxidant and antimicrobial role in the rhizosphere. Glutathione metabolism supports redox balance and detoxification, while phenylpropanoid biosynthesis reinforces cell walls. The overlap in flavonoid related pathways across both tissues suggests their central role in systemic IR activated by PPE.

3.7. Metabolomic profiling of PPE extract with LC-MS

LC-MS analysis of PPE revealed a diverse array of primary and secondary metabolites in PPE. Notably, 80 % of the identified compounds were secondary metabolites, with 65 % belonging to the polyphenol and flavonoid classes. Meanwhile, 20 % of the identified compounds were primary metabolites, including carbohydrates, organic acids, and amino acid derivatives (Table 1). Some of the identified compounds, such as rutin, naringenin, trehalose, benzoic acid, chlorogenic acid, and d-sorbitol, have previously been described to elicit a defence response in plants against a wide range of pests.

4. Discussion

This study investigated the feasibility of repurposing agricultural byproducts and waste streams to create value added products, specifically focusing on bioprotectants that induce plant resistance. Previous studies have demonstrated that agricultural byproducts such as vegetable and fruit peel extracts can function as bioprotectants by inducing resistance in plants and/or killing pathogens. Neem (*Azadirachta indica*) extracts, which contain azadirachtin, are commonly used to control pests such as aphids, whiteflies, and caterpillars in cotton, vegetables, and grain crops. Pyrethrum, derived from *Chrysanthemum cinerariifolium*, contains pyrethrins, which act as neurotoxins against a wide range of insect pests in various crops. Additionally, essential oils from garlic (*Allium sativum*) and eucalyptus (*Eucalyptus* spp.) contain bioactive compounds such as allicin and monoterpenoids, which exhibit insecticidal and antimicrobial properties (Ensley 2018; Shu et al., 2018) Extracts from cantaloupe (*Cucumis melo* var. *cantalupensis*) peels act as nematicides and induce resistance to various pathogens (De Kesel et al., 2022). The bioactive compounds in these extracts, such as ascorbic acid and its oxidised form, dehydroascorbic acid, have been demonstrated to induce resistance against Mg in rice plants (Chavan et al., 2022; De Kesel et al., 2022).

We analysed three extracts from fruit peelings of the Rosaceae family to identify potential agricultural byproducts streams that could be upcycled into effective bioprotectants. The results highlight the

Table 1
Annotated chemical constituents of PPE identified by HPLC-Q-Exactive HF-X Orbitrap mass spectrometry in negative ionization mode. The table list including chemical class, spectral similarity scores, mass-to-charge ratios (*m/z*), retention times (tR), and relative abundance (log_{10} peak area) of the identified compounds.

no	Identified compounds	Class of compound	Spectral Similarity	*m/z*	*tR*	Log_{10} Peak Area
1	Citric acid	Organic acid	0.752	191.02	0.34	7.94
2	Isoquercitrin	Flavonoid	0.926	463.09	6.24	6.88
3	Chlorogenic Acid	Polyphenol	0.916	353.09	4.69	6.86
4	Alphitolic acid	Triterpenoid	0.805	617.38	14.63	6.69
5	Kuromanin	Flavonoid	0.909	447.09	4.98	6.59
6	Rutin	Flavonoid	0.968	609.15	6.23	6.54
7	Quinic acid	Polyphenol	0.946	191.06	4.69	6.51
8	Cyanidin-3-glucoside	Flavonoid	0.878	465.10	5.12	6.48
9	Neochlorogenic Acid	Polyphenol	0.949	353.09	3.91	6.30
10	Isorhamnetin-3-O-glucoside	Flavonoid	0.932	477.10	6.86	6.18
11	Kaempferol-3-O-rutinoside	Flavonoid	0.957	593.15	6.62	6.11
12	Catechin	Flavonoid	0.949	289.07	4.54	6.08
13	Cyanidin 3-Galactoside	Flavonoid	0.846	448.10	4.98	5.95
14	Astragalin	Flavonoid	0.971	447.09	6.74	5.82
15	Baimaside	Flavonoid	0.949	625.14	5.73	5.79
16	Phenylethyl primeveroside	Glycoside	0.865	461.17	5.91	5.73
17	Benzoic acid	Organic acid	0.915	205.09	6.74	5.71
18	Tiliroside	Flavonoid	0.939	593.13	7.97	5.63
19	Abscisic acid	Plant hormone	0.788	263.13	7.69	5.63
20	Cyanidin-3-rutinoside	Flavonoid	0.910	593.15	5.13	5.59
21	Procyanidin B1	Polyphenol	0.910	577.14	4.45	5.52
22	Astragalin	Flavonoid	0.979	447.09	6.58	5.43
23	D-Sorbitol	Sugar alcohol	0.835	181.07	0.30	5.30
24	Hyperoside	Flavonoid	0.957	927.18	6.24	5.28
25	Pantothenic acid	Vitamin B5	0.976	218.10	3.39	5.26
26	Procyanidin C1	Flavonoid	0.891	865.20	4.83	5.23
27	Vanillic acid 4-beta-d-glucoside	tannin	0.939	329.09	3.68	5.20
28	Trehalose	Disaccharide	0.877	341.11	3.07	5.18
29	3-Feruloylquinic acid	Polyphenol	0.879	367.10	5.60	5.11
30	3-p-coumaroylquinic acid	Polyphenol	0.868	337.09	5.77	5.08
31	Naringenin	Flavonoid	0.925	271.06	6.86	4.89
32	Procyanidin B2	Flavonoid	0.855	577.14	5.69	4.85

potential of peach peel extract (PPE) to induce systemic resistance against *Meloidogyne graminicola* in rice plants. Our findings demonstrated that PPE foliar spray treatment significantly reduced the number of root knot nematodes, galls, and egg laying females in infected rice roots, whereas apricot peel extract (APE), and plum peel extract (PLPE) treatments had no significant effects (Fig. 1a). APE, PLPE, and PPE were also found to cause nematode mortality (Fig. 1b). These direct effects on nematode survival, combined with the systemic resistance induced in plants, position PPE as a dual action bioprotectant that directly kills nematodes while boosting the plant's natural defence mechanisms.

ROS play a crucial role in modulating the signal transduction pathways related to plant growth and defence mechanisms against biotic and abiotic stressors (Dumanović et al., 2021). Qualitative and quantitative assessments indicated that PPE induces oxidative stress signalling in treated plants. The systemic spread of ROS in PPE treated rice leaves showed a time dependent and spatial pattern, with distinct dynamics observed at varying distances from the point of treatment (POT). A faster and stronger ROS accumulation was detected close (1 cm) to the POT, and then slightly further away (3 cm). This suggests a robust ROS response originating at the POT that propagates systemically but diminishes in intensity with increasing distance (Fig. 3). The transient nature of H_2O_2 accumulation observed both by assays with the probe as well as biochemical measurements suggests a tightly regulated ROS burst that initiates defence signalling without causing prolonged stress to the plant (Dumanović et al., 2021). Such transient ROS responses are known to initiate signal transduction, and are ultimately transformed into metabolic and transcriptional responses (Mittler et al., 2022).

Transcriptomic analysis revealed that PPE treatment significantly upregulated genes associated with plant defence pathways, including those involved in JA signalling, the phenylpropanoid pathway, biosynthesis of terpenes, and responses to ROS (Table S2-S5). The upregulation of these DEGs upon PPE treatment and the accumulation of total phenolics and flavonoid content in treated leaves indicate that PPE activates local defence mechanisms in rice plants (Fig. 4 and 5). These local changes seem to activate a systemic signalling cascade that induces metabolic shifts, mainly in the phenylpropanoid pathway, throughout the plant. Noteworthy, although the total amount of flavonoids and phenolics does not change in root tissue, specific compounds over-accumulate in roots of PPE treated plants. Many compounds derived from the phenylpropanoid pathway contribute to antimicrobial activity and structural reinforcement (Dixon et al., 2002). Activation of JA in combination with phenylpropanoid induction are two general hallmarks of IR activation in rice (Desmedt et al., 2022). The role of JA of PPE-IR was further validated by JA accumulation in root of PPE treated plants and the lack of PPE-IR in a JA mutant. These results corroborate the role of JA in mediating systemic resistance (Nahar et al., 2011; Wang, Mostafa et al., 2021), and align with IR responses triggered by other stimuli such as DHA and piperonylic acid, and Cucurbitaceae extracts in rice (Chavan et al., 2022; De Kesel et al., 2022, Desmedt et al., 2022, Bao et al., 2023).

Although the salicylic acid (SA) concentration was not significantly affected by PPE at 24 hpt, SA may play a crucial role at earlier time points in the activation of defence related genes. This was evident from the upregulation of *OsWRKY45* and *OsNPR3* (non-expressor of pathogenesis-related genes), two independent regulators of the SA signalling pathways in rice (Shimono et al., 2007) at 6 hpt. OsNPR3 acts as a negative regulator of OsNPR1, indicating a negative feedback loop in response to increased SA levels. On the other hand, *OsWRKY45* is also activated by SA but activates a different set of downstream genes than NPR1. In rice, WRKY transcription factor genes are induced as early as 3 hpt in response to benzothiadiazole (BTH), a functional analogue of SA (Shimono et al., 2007). Thus, PPE treatment seems to orchestrate a coordinated defence response by activating JA and SA signalling in a time dependent manner. The enrichment of GO terms involved in DNA transcription and RNA biosynthesis at 24 hpt suggests that PPE not only activates immediate defence responses but could also prime the plant for

sustained defensive readiness. The downregulation of genes associated with chromatin assembly and DNA packing also hints at epigenetic reprogramming, where the chromatin structure is altered to activate or silence specific genes. This could allow for adaptive responses that can result in long term epigenetic changes that affect gene expression in future generations (Lämke and Bäurle 2017). This hypothesis warrants further testing of potential transmission of these defence responses to the next generation.

Untargeted metabolomics analyses on shoots of PPE treated plants reveals a local accumulation of compounds involved in defence and systemic signalling. Notable among these are resveratrol dimers, potent phytoalexins known for their antimicrobial activity (Chang et al., 2011) and 1-methylsulfinylbutenyl isothiocyanate, a glucosinolate derived compound with established nematicidal properties (Duke 2022). Simultaneously, the downregulation of key growth-related metabolites provides compelling evidence for a strategic reallocation of resources. The significant decrease in Gibberellin A11, a bioactive gibberellin that promotes stem elongation and growth (Castro-Camba et al., 2022) and Indole-3-carboxylic acid, an auxin related compound (Böttcher et al., 2014) is a clear metabolic signature of the growth defence tradeoff (Huot et al., 2014). This phenomenon, where plants suppress growth to free up energy and carbon for defence, is often mediated by the antagonistic crosstalk between JA and gibberellin (GA) signalling (Yang et al., 2012). The data strongly suggest that PPE induced JA signalling actively suppresses the GA pathway, prioritizing the production of costly defence compounds over vegetative growth. Furthermore, the downregulation of Naringenin in the shoots is particularly revealing. While seemingly counterintuitive given the activation of flavonoid biosynthesis genes, naringenin is the central precursor from which most other flavonoids are synthesized (Xu et al., 2022). Its depletion indicates a high rate of metabolic flux, where the precursor pool is being rapidly consumed and channelled into the production of various downstream flavonoid end products, signifying a pathway that is in a high catabolic state.

The root metabolome shows a distinct profile geared towards reinforcement against nematode invasion. Although the total amount of phenolics and flavonoids did not change, unbiased metabolomics revealed that the roots of PPE treated plants contain a specific arsenal of powerful phytoalexins. This includes accumulation of diterpene glycosides, a major class of defence compounds in rice that are often stored in their inactive glycosylated form until attack (Wang et al., 2018), and quercetin glycosides, flavonoids with antioxidant and antimicrobial activities (Mierziak et al., 2014). The accumulation of 1,2,6-Trigalloyl Glucose, a hydrolysable tannin, suggests reinforcement of the root cell walls, as tannins can cross link with cell wall components to form a tougher physical barrier against penetration (He 2022). Finally, the strong downregulation of glutathione in the roots provides independent, metabolic confirmation of the intense ROS burst reported in the study.

The accumulation of Azelaic acid in roots of above-ground PPE treated plants is a critical finding. Azelaic acid is a known mobile signal that travels through the plant vasculature to activate systemic acquired resistance (SAR) in distal tissues, often by priming SA accumulation (Priya Reddy and Oelmüller 2024). SAR is a specific IR phenotype induced by pathogenic organisms. The presence of Azelaic acid in the roots of PPE treated plants provides a direct mechanistic link for how the systemic signal initiated in the leaves translates to defence activation in the roots.

The KEGG pathway enrichment analysis (Fig:7c & d) provides a high-level view that seamlessly integrates the transcriptomic and metabolomic datasets. In the shoots, the enrichment of alpha linolenic acid metabolism is the direct upstream pathway for JA biosynthesis, validating the transcriptional observations of JA pathway activation and hormone accumulation. The enrichment of glycerophospholipid metabolism highlights the critical role of membrane lipids, which are hydrolysed by phospholipases to release fatty acids (like linolenic acid) that serve as precursors for defence signalling molecules (Canonne et al., 2011). In both shoots and roots, the enrichment of phenylpropanoid and flavonoid biosynthesis is consistent with the RNA seq data and the observed accumulation of phenolic compounds like caffeic acid, resveratrol, and quercetin glycoside. The enrichment of glutathione metabolism further corroborates the intense ROS activity and subsequent detoxification efforts.

Our results suggest that PPE contains unique bioactive compounds. Based on literature, peach and its peels are rich sources of bioactive primary and secondary metabolites, such as quinic acid, chlorogenic acid, fumaric acid, isoquercitrin, ascorbic acid, and other phenolic compounds, and the concentrations of these bioactive compounds are much higher in peels than in the pulp, making them more suitable for the extraction of these bioactive compounds (Gedük and Atsız 2022; Liu et al., 2015). Metabolomic analysis was executed on the here used peach peel extract to detect candidate bioactive compounds. A rich array of compounds was detected in PPE, with 80 % being secondary metabolites, predominantly polyphenols and flavonoids (65 %). Several identified compounds, including rutin, naringenin, trehalose, benzoic acid, chlorogenic acid, and D-sorbitol, have previously been described to induce defence responses in plants against a wide variety of pests (Table 1). Exogenous application of 2 mM rutin enhanced the resistance of rice, tobacco, and Arabidopsis against bacterial pathogens (*Xanthomonas oryzae, Ralstonia solanacearum*, and *Pseudomonas syringae*). This enhanced resistance was linked to earlier and stronger expression of the SA dependent defence pathway (Yang, Xu et al., 2016). Naringenin has been shown to activate immune signaling in Arabidopsis, illustrated by the induction of PR genes and induced resistance to *Pseudomonas syringae*. Mechanistically, naringenin triggers the accumulation of SA and the activation of mitogen-activated protein kinases, leading to monomerization and nuclear accumulation of the SA co-activator NPR1, which in turn drives PR gene expression (An et al., 2021). Trehalose has also been reported to activate defence enzymes and induce disease resistance in plants. For example, treating wheat with trehalose markedly enhanced its resistance to powdery mildew and this was accompanied by a higher activity of defence enzymes such as phenylalanine ammonia lyase and peroxidases (Reignault et al., 2001). Sorbitol can influence effector triggered immunity by modulating the levels of resistance proteins. In the apple *Malus domestica*, sorbitol was shown to regulate the expression of a specific resistance protein (MdNLR16) that recognizes an effector (HRIP1) from the fungus *Alternaria alternata* (Meng et al., 2018). Benzoic acid (and some hydroxylated derivatives) can induce IR against *Alternaria solani* in tomato. Specifically, benzoic acid treatment raised levels of SA and upregulated SA-biosynthetic as well as SA-responsive PR genes (*PR1, PR4, PR5*, etc.). It also boosts antioxidant enzymes and phenolic antioxidants to maintain cellular homeostasis (Nehela et al., 2021). Chlorogenic acid has been shown to increase the resistance of postharvest peach fruit to *Penicillium expansum* and increase its shelf life (Jiao et al., 2018). Further studies will be needed to identify which of these compounds, either alone or in combination, are responsible for the bioprotectant activity of PPE against nematodes.

While this study demonstrates PPE's effectiveness under controlled conditions, field application will require consideration of environmental factors such as UV exposure, temperature fluctuations, and microbial degradation that may affect the stability and persistence of bioactive compounds over time. However, these challenges can be addressed through appropriate formulation strategies, including microencapsulation techniques, stabilizing additives, or controlled-release systems that have proven successful for other plant-based bioprotectants. Such formulations could enhance compound stability, extend bioactivity duration, and improve the practical application potential of PPE under variable field conditions.

In conclusion, the findings of this study underscore the potential of PPE as an effective bioprotectant against Mg in rice. The identification of multiple defence-activating compounds provides a mechanistic basis for PPE's observed effects and suggests broader applications against other pathogens. These compounds collectively contribute to PPE's dual

action: nematicidal and IR stimulating. While JA signalling emerges as a central requirement for PPE-induced resistance, contributions from other hormones, particularly SA-related pathways should not be discounted given the complexity of plant defence networks. While the current findings establish proof of concept efficacy against root knot nematodes, subsequent research should address the spectrum of activity, field scale performance, optimisation of application methods, and further characterisation of compound synergies. Such investigations will facilitate optimised formulation strategies and mechanistic understanding required for practical implementation in integrated pest management systems, ultimately leveraging PPE's rich bioactive profile of PPE for sustainable agriculture.

CRediT authorship contribution statement

Yaseen Ahmad: Writing – original draft, Visualization, Validation, Software, Methodology, Funding acquisition, Conceptualization. **Karen De Kock:** Writing – review & editing, Supervision. **Kristof Demeestere:** Writing – review & editing. **Muhammad Nauman Ahmad:** Writing – review & editing, Supervision. **Tim De Meyer:** Writing – review & editing. **Susanne K. Wiedmer:** Writing – review & editing. **Tina Kyndt:** Writing – review & editing, Supervision, Methodology, Funding acquisition.

Declaration of competing interest

The authors declare that they have no known competing financial interests or personal relationships that could have appeared to influence the work reported in this paper.

Supplementary materials

Supplementary material associated with this article can be found, in the online version, at doi:10.1016/j.stress.2025.101113.

Data availability

Data will be made available on request.

References

An, J., et al., 2021. Naringenin induces pathogen resistance against Pseudomonas syringae through the activation of NPR1 in Arabidopsis. Front. Plant. Sci. 12, 672552.

Assadpour, E., et al., 2024. Application of essential oils as natural biopesticides; recent advances. Crit. Rev. Food. Sci. Nutr. 64 (19), 6477–6497.

Bao, Y.J., et al., 2023. Emerging role of jasmonic acid in woody plant development. Adv. Agrochem.

Bernard, G.C., Egnin, M., Bonsi, C., 2017. The impact of plant-parasitic nematodes on agriculture and methods of control. Nematol-Concepts. Diagn. Control. 10, 121–151.

Böttcher, C., et al., 2014. The biosynthetic pathway of indole-3-carbaldehyde and indole-3-carboxylic acid derivatives in Arabidopsis. Plant. Physiol. 165 (2), 841–853.

Bybd Jr, D., Kirkpatrick, T., Barker, K., 1983. An improved technique for clearing and staining plant tissues for detection of nematodes. J. Nematol. 15 (1), 142.

Canonne, J., Froidure-Nicolas, S., Rivas, S., 2011. Phospholipases in action during plant defense signaling. Plant. Signal. Behav. 6 (1), 13–18.

Castro-Camba, R., et al., 2022. Plant development and crop yield: the role of gibberellins. Plants 11 (19), 2650.

Chang, X., et al., 2011. The phytoalexin resveratrol regulates the initiation of hypersensitive cell death in Vitis cell. PloS. One 6 (10), e26405.

Chavan, S.N., et al., 2022. Dehydroascorbate induces plant resistance in rice against root-knot nematode meloidogyne graminicola. Mol. Plant. Pathol. 23 (9), 1303–1319.

Conrath, U., 2009. Priming of induced plant defense responses. Adv. Bot. Res. 51, 361–395.

Daudi, A., O'brien, J.A., 2012. Detection of hydrogen peroxide by DAB staining in Arabidopsis leaves. Bio. Protoc. 2 (18) e263-e263.

De Kesel, J., et al., 2022. Cucurbitaceae COld Peeling extracts (CCOPEs) protect plants from root-knot nematode infections through induced resistance and nematicidal effects. Front. Plant. Sci. 12, 785699.

De Kock, K., Matthys, J., Kyndt, T., 2024. ROS detection and quantification in plant–Nematode interactions. Plant-Nematode Interactions. Springer, pp. 305–316.

Desmedt, W., et al., 2021. The phenylpropanoid pathway inhibitor piperonylic acid induces broad-spectrum pest and disease resistance in plants. Plant. Cell. Env. 44 (9), 3122–3139.

Desmedt, W., et al., 2022. Distinct chemical resistance-inducing stimuli result in common transcriptional, metabolic, and nematode community signatures in rice root and rhizosphere. J. Exp. Bot. 73 (22), 7564–7581.

Dixon, R.A., et al., 2002. The phenylpropanoid pathway and plant defence—A genomics perspective. Mol. Plant. Pathol. 3 (5), 371–390.

Duke, S.O., 2022. Benefits of resveratrol and pterostilbene to crops and their potential nutraceutical value to mammals. Agriculture 12 (3), 368.

Dumanović, J., et al., 2021. The significance of reactive oxygen species and antioxidant defense system in plants: a concise overview. Front. Plant. Sci. 11, 552969.

Ensley, S.M., 2018. Pyrethrins And Pyrethroids. Veterinary Toxicology. Elsevier, pp. 515–520.

Eugui, D., et al., 2022. Glucosinolates as an effective tool in plant-parasitic nematodes control: exploiting natural plant defenses. Appl. Soil. Ecol 176, 104497.

FAO (2021). Food outlook: biannual report on global food markets. Rome, Italy.

Ge, S.X., Jung, D., Yao, R., 2020. ShinyGO: a graphical gene-set enrichment tool for animals and plants. Bioinformatics 36 (8), 2628–2629.

Gedük, A.Ş., Atsız, S., 2022. LC-MS/MS phenolic composition of peach (Prunus persica (L.) Batsch) extracts and an evaluation of their antidiabetic, antioxidant, and antibacterial activities. S. Afr. J. Bot. 147, 636–645.

Gupta, K., et al., 2021. Greenhouse gas emission from rice fields: a review from Indian context. Environ. Sci. Pollut. Re.s 28 (24), 30551–30572.

Haeck, A., et al., 2018. Trace analysis of multi-class phytohormones in Oryza sativa using different scan modes in high-resolution orbitrap mass spectrometry: method validation, concentration levels, and screening in multiple accessions. Anal. Bioanal. Chem. 410, 4527–4539.

He, H.F., 2022. Recognition of gallotannins and the physiological activities: from chemical view. Front. Nutr. 9, 888892.

Hoagland, D., 1920. Optimum nutrient solutions for plants. Science 52 (1354), 562–564.

Hodges, D.M., et al., 1999. Improving the thiobarbituric acid-reactive-substances assay for estimating lipid peroxidation in plant tissues containing anthocyanin and other interfering compounds. Planta 207, 604–611.

Huot, B., et al., 2014. Growth–defense tradeoffs in plants: a balancing act to optimize fitness. Mol. Plant 7 (8), 1267–1287.

Jamiołkowska, A., 2020. Natural compounds as elicitors of plant resistance against diseases and new biocontrol strategies. Agronomy 10 (2), 173.

Jiao, W., et al., 2018. Chlorogenic acid induces resistance against penicillium expansum in peach fruit by activating the salicylic acid signaling pathway. Food. Chem. 260, 274–282.

Kaur, N., et al., 2016. Detection of reactive oxygen species in Oryza sativa L.(rice). Bio. Protoc. 6 (24) e2061-e2061.

Kitowski, I., et al., 2020. A pesticide banned in the European Union over a decade ago is still present in raptors in Poland. Env. Conserv 47 (4), 310–314.

Koul, B., Yakoob, M., Shah, M.P., 2022. Agricultural waste management strategies for environmental sustainability. Env. Res. 206, 112285.

Kumar, V., Khan, M.R., Walia, R., 2020. Crop loss estimations due to plant-parasitic nematodes in major crops in India. Natl. Acad. Sci. Lett. 43 (5), 409–412.

Lämke, J., Bäurle, I., 2017. Epigenetic and chromatin-based mechanisms in environmental stress adaptation and stress memory in plants. Genome. Biol 18, 1–11.

Lawrence, M., et al., 2013. Software for computing and annotating genomic ranges. PLoS. Comput. Biol. 9 (8), e1003118.

Liu, H., Cao, J., Jiang, W., 2015. Evaluation and comparison of vitamin C, phenolic compounds, antioxidant properties and metal chelating activity of pulp and peel from selected peach cultivars. LWT-Food. Sci. Technol. 63 (2), 1042–1048.

Mahapatra, B., et al., 2021. Aerobic Rice and its significant perspective for sustainable crop production. Indian. J. Agron 66 (4), 383–392.

Mantelin, S., Bellafiore, S., Kyndt, T., 2016. Meloidogyne graminicola: a major threat to rice agriculture. Mol. Plant. Pathol. 18 (1), 3.

Martínez-Medina, A., et al., 2017. Shifting from priming of salicylic acid-to jasmonic acid-regulated defences by Trichoderma protects tomato against the root knot nematode Meloidogyne incognita. New. Phytol. 213 (3), 1363–1377.

Meng, D., et al., 2018. Sorbitol modulates resistance to Alternaria alternata by regulating the expression of an NLR resistance gene in apple. Plant. Cell 30 (7), 1562–1581.

Miersch, O., et al., 2008. Hydroxylated jasmonates are commonly occurring metabolites of jasmonic acid and contribute to a partial switch-off in jasmonate signaling. New. phytol 177 (1), 114–127.

Mierziak, J., Kostyn, K., Kulma, A., 2014. Flavonoids as important molecules of plant interactions with the environment. Molecules 19 (10), 16240–16265.

Mittler, R., et al., 2022. Reactive oxygen species signalling in plant stress responses. Nat. Rev. Mol. Cell. Boil. 23 (10), 663–679.

Nahar, K., et al., 2011. The jasmonate pathway is a key player in systemically induced defense against root knot nematodes in rice. Plant. Physiol. 157 (1), 305–316.

Nehela, Y., et al., 2021. Benzoic acid and its hydroxylated derivatives suppress early blight of tomato (Alternaria solani) via the induction of salicylic acid biosynthesis and enzymatic and nonenzymatic antioxidant defense machinery. J. Fungi. 7 (8), 663.

Nikolaeva, T., Lapshin, P., Zagoskina, N., 2022. Method for determining the total content of phenolic compounds in plant extracts with Folin–Denis reagent and Folin–Ciocalteu reagent: modification and comparison. Russ. J. Bioorg. Chem. 48 (7), 1519–1525.

O'Brien, J.A., et al., 2012. Reactive oxygen species and their role in plant defence and cell wall metabolism. Planta 236, 765–779.

Patro, R., et al., 2017. Salmon provides fast and bias-aware quantification of transcript expression. Nat. Methods 14 (4), 417–419.
Priya Reddy, Y., Oelmüller, R., 2024. Lipid peroxidation and stress-induced signalling molecules in systemic resistance mediated by azelaic acid/AZELAIC ACID INDUCED1: signal initiation and propagation. Physiol. Mol. Biol. Plants 30 (2), 305–316.
Rani, L., et al., 2021. An extensive review on the consequences of chemical pesticides on human health and environment. J. Clean. Prod 283, 124657.
Ravindra, H., et al., 2017. Rice root-knot nematode (Meloidogyne graminicola) an emerging problem. Int. J. Curr. Microbiol. Appl. Sci. 6 (8), 3143–3171.
Reignault, P., et al., 2001. Trehalose induces resistance to powdery mildew in wheat. New. Phytol. 149 (3), 519–529.
Riemann, M., et al., 2003. Impaired induction of the jasmonate pathway in the rice mutant hebiba. Plant. Physiol. 133 (4), 1820–1830.
Schmid, R., et al., 2023. Integrative analysis of multimodal mass spectrometry data in MZmine 3. Nat. Biotechnol. 41 (4), 447–449.
Shah, S.M.Z., et al., 2023. Untargeted screening of plant metabolites based on data-independent and data-dependent acquisition modes using LC-ESI-QTOF-MS: tribulus terrestris L. as a case study. Arab. J. Chem. 16 (8), 104978.
Shimono, M., et al., 2007. Rice WRKY45 plays a crucial role in benzothiadiazole-inducible blast resistance. Plant. Cell 19 (6), 2064–2076.
Shraim, A.M., et al., 2021. Determination of total flavonoid content by aluminum chloride assay: a critical evaluation. Lwt 150, 111932.
Shu, B., et al., 2018. Azadirachtin affects the growth of Spodoptera litura Fabricius by inducing apoptosis in larval midgut. Front. Physiol 9, 137.
Slusarenko, A.J., Patel, A., Portz, D., 2008. Control of plant diseases by natural products: allicin from garlic as a case study. Sustain. Dis. Manag. Eur. Context 313–322.
Song, P., et al., 2021. Natural phytoalexin stilbene compound resveratrol and its derivatives as anti-tobacco mosaic virus and anti-phytopathogenic fungus agents. Sci. Rep. 11 (1), 16509.
Takeda, H., et al., 2024. MS-DIAL 5 multimodal mass spectrometry data mining unveils lipidome complexities. Nat. Commun. 15 (1), 9903.
Tapia-Vázquez, I., et al., 2022. Root-knot nematodes (Meloidogyne spp.) a threat to agriculture in Mexico: biology, current control strategies, and perspectives. World. J. Microbiol. Biotechnol. 38 (2), 26.
Varma, V.S., et al., 2015. Potential of waste carbide sludge addition on earthworm growth and organic matter degradation during vermicomposting of agricultural wastes. Ecol. Eng. 83, 90–95.
Wang, B., et al., 2016. Advances in recycling and utilization of agricultural wastes in China: based on environmental risk, crucial pathways, influencing factors, policy mechanism. Procedia. Env. Sci. 31, 12–17.
Wang, W., et al., 2018. Rice secondary metabolites: structures, roles, biosynthesis, and metabolic regulation. Molecules 23 (12), 3098.
Wang, Y., et al., 2021. Function and mechanism of jasmonic acid in plant responses to abiotic and biotic stresses. Int. J. Mol. Sci. 22 (16), 8568.
Whitehead, A., Hemming, J., 1965. A comparison of some quantitative methods of extracting small vermiform nematodes from soil. Ann. appl. Biol. 55 (1), 25–38.
Xu, H., et al., 2022. AfCHIL, a type IV chalcone isomerase, enhances the biosynthesis of naringenin in metabolic engineering. Front. Plant. Sci. 13, 891066.
Yang, D.L., et al., 2012. Plant hormone jasmonate prioritizes defense over growth by interfering with gibberellin signaling cascade. Proc. Natl. Acad. Sci. 109 (19). E1192-E1200.
Yang, W., et al., 2016. Rutin-mediated priming of plant resistance to three bacterial pathogens initiating the early SA signal pathway. PloS. One. 11 (1), e0146910.
Yang, Z., et al., 2023. Population dynamics of meloidogyne graminicola in soil in different types of direct-seeded rice agroecosystems in Hunan Province, China. J. Nematol. 55 (1).